**Proceedings ICFDP7:**
**Seventh International Congress on Fluid Dynamics and Propulsion**
**18–20 December 2001, Cairo, Egypt**

**ICFDP7-2001039**

# SPATIO–TEMPORAL STABILITY OF FLOW THROUGH COLLAPSIBLE TUBES

M. Hamadiche
LMFA, Ecole Centrale de Lyon
69131 Ecully CEDEX, France
<hamadich@mecaflu.ec-lyon.fr>

M. Gad-el-Hak
Department of Aerospace & Mechanical Engineering
University of Notre Dame
Notre Dame, IN 46556, U.S.A.
<gadelhak@nd.edu>

## ABSTRACT

The stability of the Hagen–Poiseuille flow of a Newtonian fluid in an incompressible, collapsible, viscoelastic tube is determined using linear stability analysis. A novel numerical strategy is introduced to study the spatio–temporal stability of the coupled fluid–structure system subjected to infinitesimal axisymmetric or non-axisymmetric disturbances. The strategy alleviates the need for an initial guess and thus ensures that all the unstable modes within a given closed region in the complex eigenvalue plane will be found. The stiff nature of the governing equations dictated the use of the method of renormalization (Scott and Watts, 1977) in order to achieve rapid convergence. The parameters of the system are chosen such that it is stable if the compliant duct is not allowed to collapse, in this way any unstable mode found is expected to be unique to collapsible tubes. Three different unstable modes are found and the present results are in excellent agreement with existing experiments. The non-axisymmetric, low-frequency unstable mode represents an absolute instability, while the other two unstable modes, one high- and one low-frequency, are convective instabilities.

## INTRODUCTION

Fluid conduits which are capable of collapse are commonly found in nature as well as in man-made systems. Although it may not be desirable for collapse to actually commence, numerous applications necessitate the use of soft tubing, in contrast to rigid pipes. Engine, fire and garden hoses, and many of the tubes used for medical and laboratory applications are made of elastic or viscoelastic materials and are designed so that collapse does not occur under normal operating conditions. In other applications, such as peristaltic pumps, blood transfusion and assisted breathing, controlled collapsing is part of the design objective.

All fluid-carrying conduits in humans and other mammals are flexible and can collapse under sufficiently negative transmural pressure (internal pressure minus external pressure). Examples of tubes that can collapse as a result of trauma or disease are blood vessels, bronchial airways and the gut. Conduits that do collapse during their normal operation include intra-myocardial coronary blood vessels during systole, pulmonary blood vessels in the upper parts of the lung, large airways during forced expiration, urethra during micturition, and glottis during phonation.

Internal pressure decreases along a constant-area duct, so such tube tends to collapse at the downstream end if the pressure external to the tube is sufficiently large. For a prescribed external and inlet pressures and fluid and tube types, collapse will occur as the exit pressure is reduced in order to effect higher flow rates (i.e. higher Reynolds numbers). When collapsed, the cross-section of a round tube becomes highly non-circular and the flow rate is significantly reduced or even stopped, certainly the reverse of what is intended. Two types of collapse are typically encountered, one in which the throat area asymptotes to a minimum and the resulting flow is steady, and the other where the throat area and axial position, flow rate, and exit conditions oscillate periodically or even chaotically despite constant supply conditions. Oscillating collapsible tubes are less common in vivo but are nevertheless observed when a vocal cord vibrates or when a brachial artery is compressed by a sphygmomanometer cuff, resulting in the so-called Korotkoff sound.

Because of their importance in medicine as well as technology and their intrinsic interest as complex dynamical systems, collapsible tubes have been extensively studied experimentally (Bertram and Castles, 1999; Kounanis and Mathioulakis, 1999; and references therein) as well as analytically and numerically (Shapiro, 1977; Heil, 1997; Luo and Pedley, 2000; and references therein). The goal of these researches is to understand the phenomenon of collapse in order to prevent, control or exploit it.


Copyright © 2001 by ASME

## Prior Experiments

In controlled experiments, a uniform flexible tube is typically mounted between two rigid pipes in a so-called Starling resistor configuration. The supply pressure is varied and the pressure external to the compliant tube is controlled by surrounding the tube with a larger pressurized chamber. Observations are made of the collapse process (i.e. non-axisymmetric buckling) and any accompanied oscillations in the throat area, the flow rate and the exit pressure. Several non-invasive techniques have been developed to record the tube geometry during collapse, for example X-ray cinefluorography, stereophotogrammetric methods, magnetic resonance imaging, ultrasound imaging, tomography, and coded raster imaging. Though invasive, conductimetric catheterization can be used to provide accurate time-dependent cross-sectional area of a collapsible tube during strictly repetitive oscillations. In a totally different setting, the conductance catheter method is used widely to monitor in vivo the changing volume of heart chambers.

Bertram and Godbole (1995) used conductimetric catheterization to measure the instantaneous, shape-independent area at incrementally adjusted positions along the length of a collapsed, periodically oscillating tube. They observed three distinct modes of oscillations with sharp, discontinuous transitions separating them. Bertram and Godbole termed the two low-frequency modes *LU* and *LD*, and the intermediate-frequency mode *I*. The low-frequency modes are distinguished by waveform shape: for *LU*, the collapse is brief relative to cycle length and is followed by a phase of relative quiescence; and for *LD*, the collapse lasts for approximately half the period. The third mode *I* has approximately three times the frequency of the other two and is obtained by transition from the brief-collapse mode as the appropriate parameter is varied. If the upstream pressure $p_u$ is held constant, *LU* is the first mode observed as the downstream transmural pressure $p_{de}=p_d - p_e$ is lowered to the point where collapse occurs and oscillations start, where $p_d$ is the pressure at the downstream end of the tube, and $p_e$ is the pressure in the chamber surrounding the tube. Further reduction of $p_{de}$ leads to either *LD* oscillations, at moderate $p_u$, or *I* oscillations at higher $p_u$.

## Present Work

In the present research, we take the view that collapse and oscillations can be the climactic manifestation of an instability of the coupled fluid–tube system. Therefore, we study the linear stability of the system prior to the onset of actual collapse. This approach clearly excludes the complex flow associated with the geometry of a non-circular, convergent–divergent nozzle and the oscillations due to the choking phenomenon, but allows us to investigate a first-principles system much more general and less ad hoc than that afforded by the lumped-parameter or the one- or two-dimensional models.

We start with a distended, constant-diameter tube made of viscoelastic material with fully-developed laminar flow inside, as shown schematically in Figure 1. The Navier–Stokes equations describe the fluid side, and the Navier equation

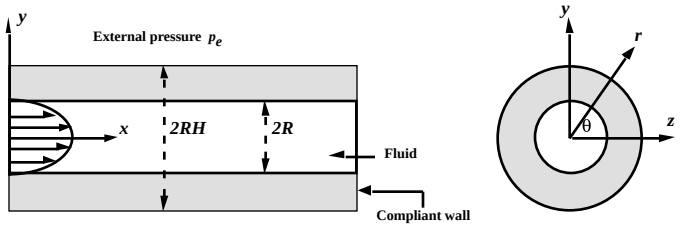


**Figure 1. System configuration.**

describes the compliant tube side. The Hagen–Poiseuille flow, the constant pressure gradient inside, the external pressure, and the tube thickness and viscoelastic properties are all specified as a basic state of the coupled dynamical system.

It is assumed that for each specified set of parameters, all the forces resulting from the steady flow, the tube stiffness and the external pressure are initially in static equilibrium to yield a constant-diameter, motionless tube capable of deforming when perturbed. We subject the coupled fluid–tube system to axisymmetric as well as non-axisymmetric perturbations and study the spatio–temporal instability (Huerre and Monkewitz, 1990; Yeo et al., 1999) of that dynamical system. The linearized Navier–Stokes and Navier equations are coupled via proper boundary conditions at the fluid–solid interface and describe the early stages of the imposed perturbation dynamics. Both inertial and viscous forces are retained in the formulation, allowing for an arbitrary Reynolds number.

The present work is a natural extension of our previous study of the stability of non-collapsible, soft tubes reported in a companion paper in these proceedings and in more details in Hamadiche and Gad-el-Hak (2001a). There, a rigid shell surrounds the compliant tube thus preventing collapse while admitting other types of tube deformation. The primary difference in formulation of the original study and the present one is therefore in the boundary condition at the outer surface of the viscoelastic tube: motionless compliant–rigid interface in the former study, and no stresses, except for the imposed time-independent external pressure, at the free surface in the new study. A second difference is that we study in here the spatio–temporal instability of the system while in the original paper we considered only the temporal instability. The present extension will allow us to make precise determination of whether a particular instability is absolute or convective.

The parameters of the present system are chosen such that it is stable if the compliant duct is not allowed to collapse, in this way any unstable mode found is expected to be unique to collapsible tubes. We utilize the same numerical method introduced in Hamadiche and Gad-el-Hak (2001a) to study—without a need for an initial guess—the stability of the coupled fluid–structure system. More details of the collapsible tube case can be found in the article by Hamadiche and Gad-el-Hak (2001b).

## RESULTS

We have used the numerical strategy used by Hamadiche and Gad-el-Hak (2001a) to study the spatio–temporal stability of the coupled fluid–tube system depicted in Figure 1 and


Copyright © 2001 by ASME

subjected to infinitesimal axisymmetric or non-axisymmetric disturbances. Three different unstable modes unique to collapsible tubes are found. Two of the unstable modes have similar amplification rate as well as approximately the same frequency which is about a third of the frequency of the third mode at the most unstable wavenumber. Moreover, the high-frequency mode is non-axisymmetric with azimuthal wavenumber $n$=1, while one of the low-frequency modes is axisymmetric *(n=0)* and the other one non axisymmetric *(n=1)*. The non-axisymmetric, low-frequency mode represents an absolute instability that results from the coalescence of a downstream and an upstream travelling wave, while the other two modes are convective instabilities. In this section, we verify the nature of those instability modes and describe their dependence on the problem parameters.

In their experiment with collapsible tubes, Bertram and Godbole (1995) and Bertram and Castles (1999) observed three distinct modes of oscillations with sharp, discontinuous transitions separating them. They termed the two low-frequency modes *LD* and *LU*, and the intermediate-frequency mode *I*. The two low-frequency modes are distinguished by waveform shape: collapse which lasts for approximately half the period for *LD*, and brief collapse relative to cycle length for *LU*. The third mode *I* had approximately three times the frequency of the other two and is obtained by transition from the brief-collapse mode as the appropriate parameter is varied.

The present results compare most favorably to the experiments of Bertram and Castles (1999). We therefore adopt the terminology used by these authors by naming the three modes found in our analysis *LD*, *LU*, and *I*. Our terminology for the high- (or intermediate-)frequency mode is clear at the outset. Which of the low-frequency modes should be called *LD* and which *LU* will become clear as we discuss the effect of external pressure on the system stability. It should be noted, however, that the modes discovered in our analysis are linear instabilities of a constant-diameter tube. Of course, the ultimate wave form cannot be predicted by our linear analysis. The experiments dealt with the large-amplitude, often-skewed oscillations of a tube that underwent actual collapse. The two situations are different to be sure, but we submit that collapse and nonlinear oscillations *can* be the climactic manifestation of a linear instability of the coupled fluid–tube system. Similarities between the linear modes in the present analysis and the experimentally observed nonlinear oscillations support our premise.

We first determined whether a particular instability mode is convective or absolute using the Spatio–temporal stability analysis described in Kupfer et al. (1987). We plotted the Laplace contours in the complex frequency plane for all three modes searching for cusp points. Figures 2a, 2b and 2c show the typical results for, respectively, modes *LD*, *I* and *LU*. As is clear, there are no cusp points in the Laplace contours in Figures 2a and 2b, indicating that the *LD* and *I* instabilities are convective. In contrast, a cusp point is seen in Figure 2c for $k_i$=0.7, indicating that the *LU* instability is absolute. This is confirmed by the appearance of a pinch point in the Fourier contours in the complex wavenumber plane depicted in Figure 2d for the same *LU* instability. The pinch point occurs at $k_r$=1.1 and $k_i$=0.7, and is of course a saddle point in the dispersion relation corresponding to the absolute instability *LU*.

In the next six figures we show the dependence of the three instability modes on the problem five dimensionless parameters: external pressure $P_e$; Reynolds number $Re$; tube stiffness $\Gamma$; tube thickness $H$; and ratio of tube viscosity to fluid viscosity $\mu_r$. The dimensionless external pressure is defined thus $P_e=(p_e - p_u)/G$, where $p_e$ is the (dimensional) external pressure, $p_u$ is the upstream pressure (at the tube inlet), and $G$ is the tube's shear modulus. We take the wavenumber $k$ to be real and the frequency $s$ to be complex, in other words we confine the results from now on to the temporal stability of the coupled system. In all six figures, *LD* will be denoted by a solid line, *LU* denoted by a broken line, and *I* denoted by a dotted line. Table 1 summarizes the key characteristics of the three instability modes.

Figures 3a and 3b show the temporal amplification rate $s_r$ and the frequency $s_i$ of the three unstable modes versus the external pressure $P_e$. The axisymmetric mode *LD* is stabilized as the external pressure is increased, while the non-axisymmetric mode *I* is stabilized as the external pressure is lowered. The non-axisymmetric, absolute instability *LU* remains unstable in the entire range of external pressures tested. For negative external pressures, the amplification rate of the axisymmetric mode *LD* is slightly higher than that for the non-axisymmetric mode *LU*, but that trend is dramatically reversed for $P_e$>0. For positive $P_e$, except for a small region around $P_e$=0, mode *I* has the highest amplification rate followed by the other non-axisymmetric mode *LU*. These observations are consistent with tube collapsing non-axisymmetrically under the influence of high external pressure, but blowing out axisymmetrically under sufficiently low external pressure. For moderately positive $P_e$, mode *LU* has the highest amplification rate which is consistent with the experimental observations of Bertram and Castles (1999).

As shown in Figure 3b, the frequency of *LD* mode and *LU* mode is about the same in the range of external pressures where both are unstable. For positive external pressure, the frequency of *I* is about three times that of *LU*. It is noteworthy that the external pressure was always positive in the experiments of Bertram and Godbole (1995), and in fact in all similar experiments using Starling resistor configuration.

Figures 4a and 4b show the temporal amplification rate and the frequency of the three unstable modes versus the real wavenumber. The peak amplification rate of the two low-frequency modes *LD* and *LU* is slightly higher than that for the high-frequency mode *I* and occurs at lower wavenumber (longer wavelength). Modes *LD* and *LU* are stabilized for $k_r$>7.5, while mode *I* is stabilized at slightly higher wavenumber. The frequency of *LD* is the same as that for *LU* in the entire range of wavenumbers tested, with both frequencies increasing monotonically as the wavenumber increases. At the most unstable wavenumbers, the frequency of mode *I* is three times


Copyright © 2001 by ASME

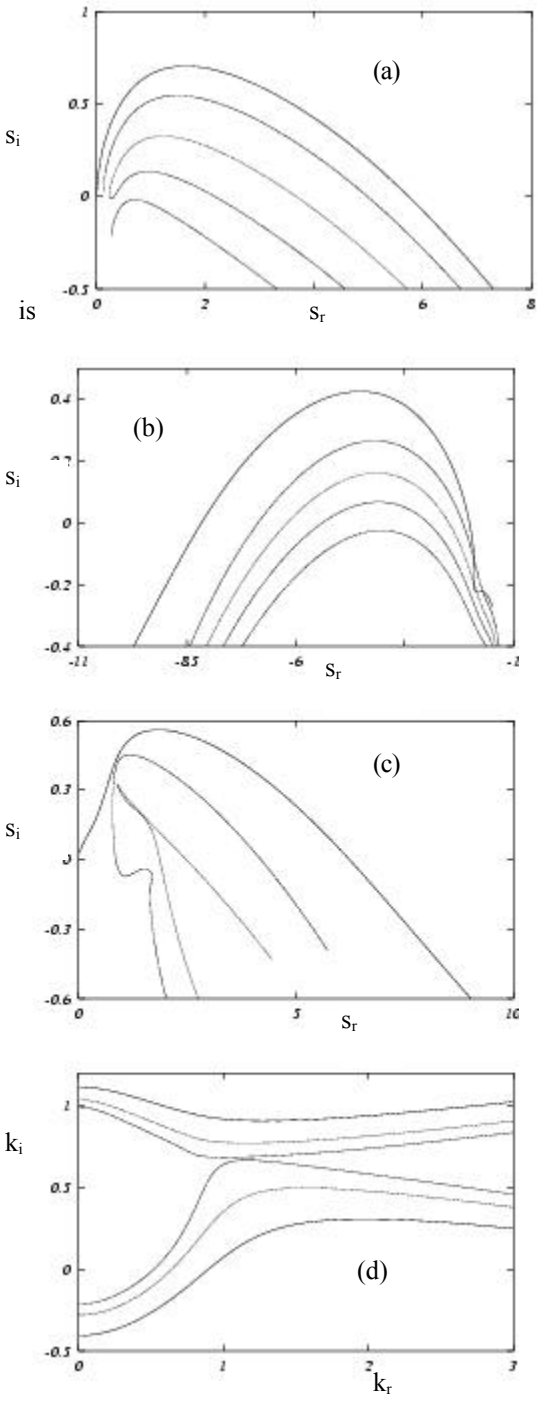


**Figure 2. Laplace and Fourier contours for the three instability modes; $P_e$=0, $Re$=50, Γ=1, $H$=1.1, $\mu_r$=0. (a) Laplace contours for the axisymmetric mode *LD*; $n$=0. Images of deformed Fourier contours are from above for $k_i$=0.0,0.2,0.5,0.8,1.1. (b) Laplace contours for the non-axisymmetric mode *I*; $n$=1. Images of deformed Fourier contours are from above for $k_i$=0.0, -0.09,-0.2,-0.3,-0.4. (c) Laplace contours for the non-axisymmetric mode *LU*; $n$=1. Images of deformed Fourier contours are from above for $k_i$=0.0, 0.39,0.7. (d) Fourier contours corresponding to mode *LU* near the saddle point. Images of deformed Laplace contours are from the outside for $s_r$=0.5,0.4,0.33.**

| | Mode *LD* | Mode *LU* | Mode *I* |
|---|---|---|---|
| Line type in Figures 3–8 | Solid line ———— | Broken line ---------- | Dotted line …… |
| Symmetry | Axi-symmetric | Non-axi-symmetric | Non-Axi-symmetric |
| Azimuthal wavenumber | $n$=0 | $n$=1 | $n$=1 |
| Frequency | Low | Low | High |
| Nature of stability | Convective | Absolute | Convective |
| Effect of external pressure | Stabilizing | Unstable for all $P_e$ | Destabilizing |

**Table 1. Summary of all three instability modes.**

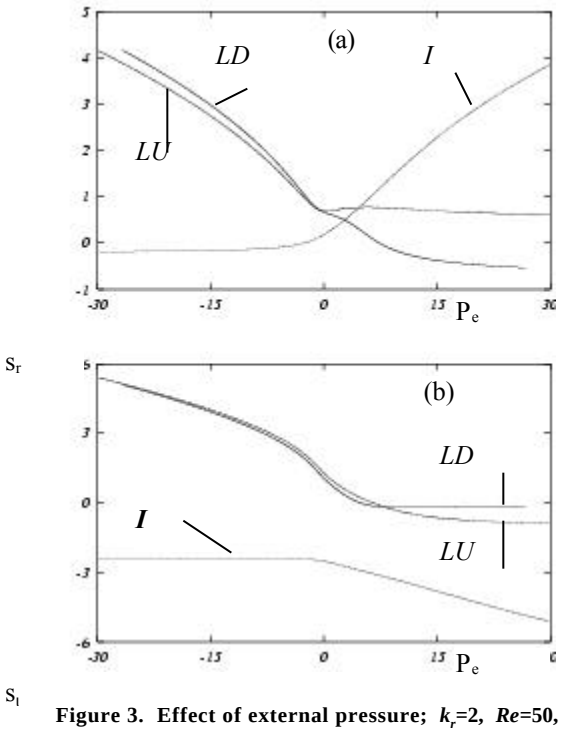


**Figure 3. Effect of external pressure; $k_r$=2, $Re$=50, Γ=1, $H$=1.1, $\mu_r$=0. (a) Amplification rate. (b) Frequency.**

that for *LD* and *LU*, in excellent agreement with the experiments of Bertram and Castles (1999).

The quasi-linear variation of the frequency with the wavenumber depicted in Figure 4b indicates the non-dispersive character of all three unstable modes. The group velocity is readily obtained by measuring the slope in Figure 4b and is approximately 0.8 in the linear region. Since $\Gamma=(\rho V^2/G)^{1/2}=1$ in this particular calculations, a group velocity of 0.8 times the maximum velocity in the pipe indicates a sub-critical perturbation, i.e. below that necessary for the onset of choking and flow limitation. For very small values of the wavenumber, $k_r$=0.25, the group velocity of the absolute instability *LU* is small but not zero. It is known that the group velocity of an


Copyright © 2001 by ASME

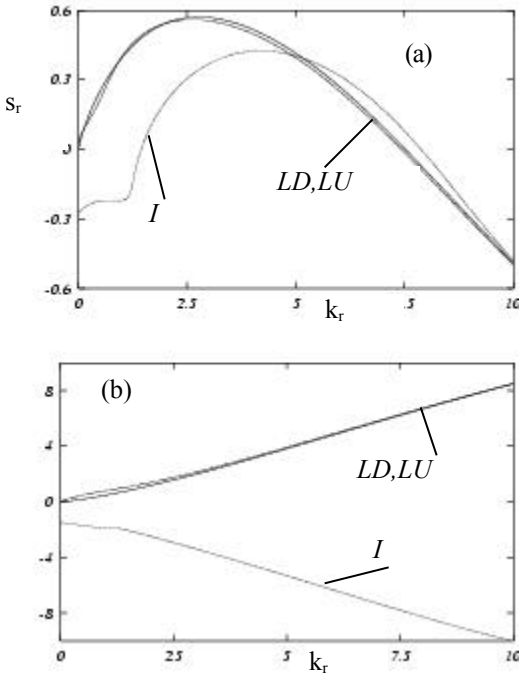


**Figure 4. Changes of the complex frequency versus real wavenumber; $P_e$=0, $Re$=100, Γ=1, $H$=1.1, $\mu_r$=0. (a) Amplification rate. (b) Frequency.**

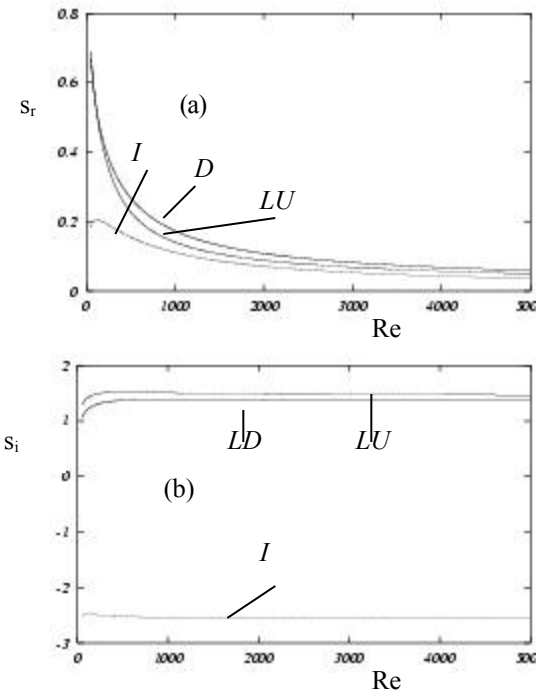


**Figure 5. Changes of the complex frequency versus Reynolds number; $k_r$=1 $P_e$=0, $Re$=50, Γ=1, $H$=1.1, $\mu_r$=0. (a) Amplification rate. (b) Frequency.**

absolute instability is zero at the pinch point $k_r$=1.1 (see Figure 2d) but not necessarily elsewhere in the complex wavenumber plane.

The quasi-linear variation of the frequency with the wavenumber depicted in Figure 4b indicates the non-dispersive character of all three unstable modes. The group velocity is readily obtained by measuring the slope in Figure 4b and is approximately 0.8 in the linear region. Since $\Gamma=(\rho V^2/G)^{1/2}=1$ in this particular calculations, a group velocity of 0.8 times the maximum velocity in the pipe indicates a sub-critical perturbation, i.e. below that necessary for the onset of choking and flow limitation. For very small values of the wavenumber, $k_r$=0.25, the group velocity of the absolute instability *LU* is small but not zero. It is known that the group velocity of an absolute instability is zero at the pinch point $k_r$=1.1 (see Figure 2d) but not necessarily elsewhere in the complex wavenumber plane.

Figures 5a and 5b show the temporal amplification rate and the frequency of the three unstable modes versus the Reynolds number. All three modes remain unstable at the highest Reynolds number tested, although the amplification rate decreases monotonically with *Re*. Although not shown in the zoomed out Figure 5a, the modes are stable for $Re$<50. The axisymmetric mode *LD* has consistently higher amplification rate followed by the azimuthally-varying mode *LU*. The high-frequency mode *I* has the lowest amplification rate. The frequencies of *LD* and *LU* are very close and is a third of the frequency of the high-frequency mode *I* in the entire range of Reynolds numbers tested, in agreement with the experimental observations of Bertram and Castles (1999).

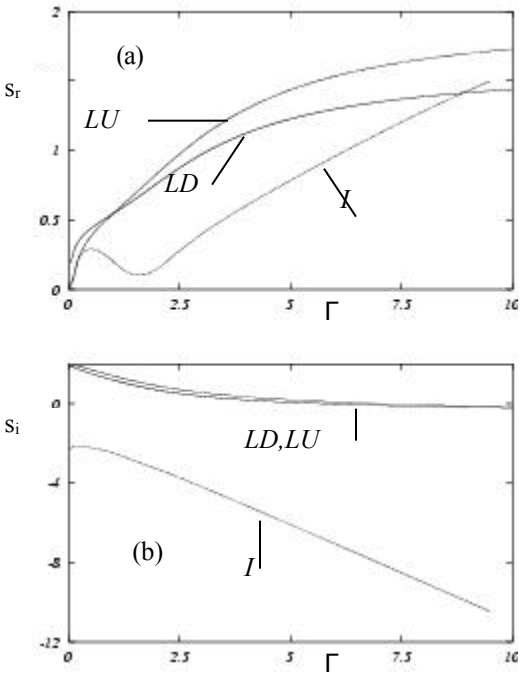


**Figure 6. Changes of the complex frequency versus coating stiffness; $k_r$=1, $P_e$=0, $Re$=100, $H$=1.1, $\mu_r$=0. (a) Amplification rate. (b) Frequency.**


Copyright © 2001 by ASME

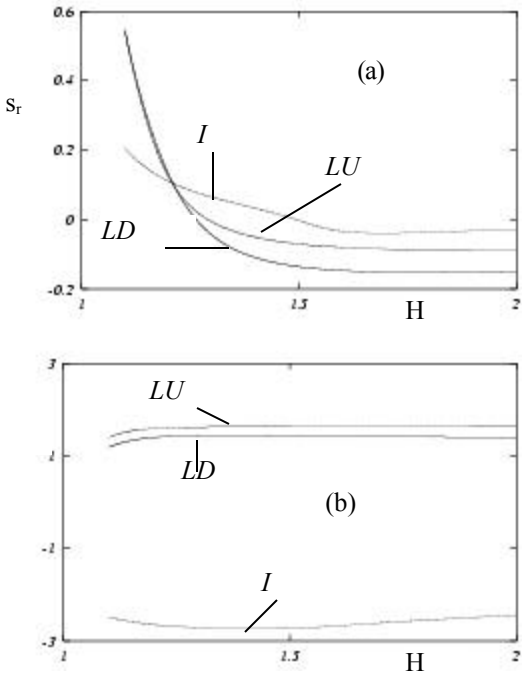


**Figure 7. Effect of coating thickness; $k_r$=2, $P_e$=0, $Re$=100, Γ=1, $\mu_r$=0. (a) Amplification rate. (b) Frequency.**

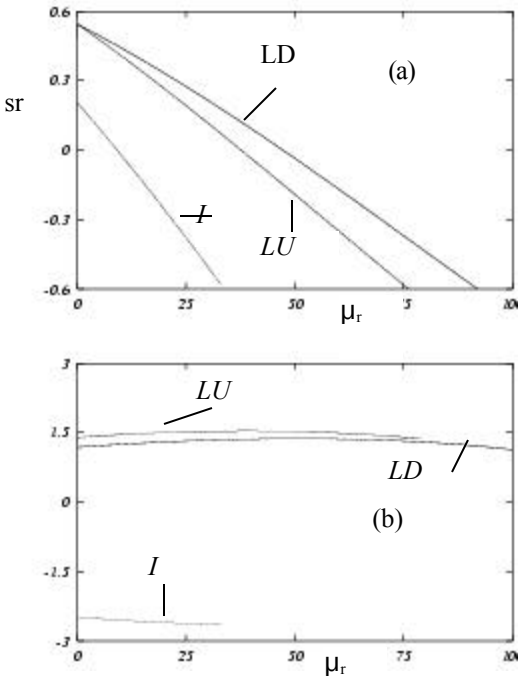


**Figure 8. Effect of coating dissipation; $k_r$=2, $P_e$=0, $Re$=100, Γ=1, $H$=1.1. (a) Amplification rate. (b) Frequency.**

Figures 6a and 6b show the temporal amplification rate and the frequency of the three unstable modes versus the dimensionless coating stiffness. As Γ goes to 0, the coating stiffens and the three modes are, as expected, stabilized. When Γ<<1, the flow velocity $V$ is much lower than the wave propagation velocity in the solid $(G/\rho)^{1/2}$, and the flow is subcritical. The azimuthally-varying instabilities *LU* and *I* stabilize sooner than the axisymmetric instability *LD* which persists to very low values of Γ. Not unexpectedly, the amplification rate for modes *LD* and *LU* increases monotonically as the coating becomes more compliant (i.e. Γ increases). Curiously, however, the amplification rate for mode *I* has both a maximum (at Γ approximately equal 0.5) and a minimum ( at Γ approximately equal 1.7).

As shown in Figure 6b, the frequency of modes *LD* and *LU* is about the same for the entire range of Γ tested. But that frequency is a third of the frequency of mode *I* only when Γ is close to 1. The ratio of the high and low frequencies increases monotonically as Γ increases, i.e. as the characteristic flow speed exceeds the characteristic propagation speed in the solid medium and the flow becomes supercritical. It has been shown by Hamadiche (1998) that in rigid wall tubes, the frequency of the eigenmode is $s_i/\Gamma$ which, according to figure 5b, goes to infinity when Γ goes to zero. Thus, in the limit of rigid wall tube, the frequency of the unstable modes goes to infinity, and all three modes can therefore be classified as solid-based, flow-induced surface instabilities, existing only as a consequence of the tube compliance.

Figure 7a shows the effect of the thickness of the elastic wall on the stability of the system. Increasing the thickness of the coating stabilizes all three modes. As compared to the two low-frequency modes *LD* and *LU*, the high-frequency mode *I* persists to a coating thickness of 50% of the tube radius. In non-collapsible tubes, decreasing the thickness of the compliant coating to zero leaves a rigid shell and therefore leads to a stable fluid–solid system. In the present collapsible tube case, in contrast, asymptoting the thickness toward zero leads to a more easily deformable tube and is therefore destabilizing, consistent with the results depicted in Figure 7a. Figure 7b shows that the frequency of modes *LD* and *LU* is about the same for the entire range of coating thicknesses tested. Mode *I* maintains the factor of three higher frequency for all thicknesses even when those modes are stable.

Figures 8a and 8b show the temporal amplification rate and the frequency of the three unstable modes versus the viscosity of the viscoelastic wall. All three modes are stabilized by increased dissipation in the solid. The high-frequency, convective mode *I* is the first to be damped by the viscosity of the solid, followed by the absolute mode *LU*, and finally the low-frequency, convective mode *LD*. Dissipation in the coating has, therefore, stronger damping effect on the non-axisymmetricinstability modes that eventually may lead to tube collapse. The frequencies of *LD* and *LU* are very close and is a third of the frequency of the high-frequency mode *I* in the entire range of coating viscosity tested, consistent with the experimental observations of Bertram and Castles (1999) who tested only a single viscoelastic coating.


Copyright © 2001 by ASME

The effect of coating viscosity shown here is not unlike that observed in zero-pressure-gradient, turbulent-boundary-layer flows over compliant coatings (see Carpenter, 1990). In a sequence of experiments, Gad-el-Hak (1986) observed that the convective traveling-wave flutter (class **B**) was stabilized by damping and appeared only in mostly elastic coatings void of any dissipation, e.g. common household gelatin. The absolute, static-divergence waves (class **C**) have higher threshold velocity as compared to flutter and did not appear in elastic coatings. For highly damped coatings, as for example PVC plastisols, the flutter was stabilized and only divergence was observed there. The absolute, divergence waves are largely unaffected by coating dissipation. In here, the coating dissipation does indeed stabilize most pronouncedly the non-axisymmetric, high-frequency mode *I*. All three modes are stabilized by the coating viscosity and, according to the energy classification of Landahl (1962), can perhaps be classified as class **B**.

## CONCLUSIONS

Fluid conduits which are capable of collapse are commonly found in nature as well as in man-made systems. A tube typically buckles non-axisymmetrically and, under steady supply conditions, the throat area may reach a new lower asymptote or may oscillate periodically or even chaotically. Understanding this complex dynamics is important and will enable the designer of soft tubes to prevent, control or exploit the collapse phenomenon. In the present research, we advanced the view that collapse and oscillations can be the climactic manifestation of an instability of the coupled fluid–tube system. We therefore studied the linear stability of the system prior to the onset of actual collapse. This approach clearly excluded the complex flow associated with the geometry of a non-circular, convergent–divergent nozzle and the oscillations due to the choking phenomenon, but allowed us to investigate a first-principles system much more general and less ad hoc than that afforded by the lumped-parameter or the one- or two-dimensional models. Similarities between the linear modes in the present analysis and the experimentally observed nonlinear oscillations supported our premise.

The stability of the Hagen–Poiseuille flow of a Newtonian fluid in an incompressible, collapsible, viscoelastic tube was determined using linear stability analysis. A novel numerical strategy was introduced to study the spatio–temporal stability of the coupled fluid–structure system subjected to infinitesimal axisymmetric or non-axisymmetric disturbances. The strategy alleviated the need for an initial guess and thus ensured that all the unstable modes within a given closed region in the complex eigenvalue plane would be found. The stiff nature of the governing equations dictated the use of the method of renormalization in order to achieve rapid convergence. The dimensionless parameters investigated were the external pressure, the Reynolds number, and the tube stiffness, its thickness and its viscosity. The parameters of the system were chosen such that it is stable if the compliant duct is not allowed to collapse, in this way any unstable mode found is expected to be unique to collapsible tubes.

Three different unstable modes were found and the present results are in excellent agreement with existing experiments. All three modes are solid-based, flow-induced surface instabilities. Two of the unstable modes have similar amplification rates as well as approximately the same frequency which is about a third of the frequency of the third mode at the most unstable wavenumber. Moreover, the high-frequency mode is non-axisymmetric with azimuthal wavenumber $n$=1, while one of the low-frequency modes is axisymmetric *(n=0)* and the other one non-axisymmetric *(n=1)*. The non-axisymmetric, low-frequency mode represents an absolute instability that results from the coalescence of a downstream and an upstream travelling wave, while the other two modes are convective instabilities.

The axisymmetric, low-frequency mode is stabilized as the external pressure is increased, while the high frequency mode is stabilized as the external pressure is lowered. The non-axisymmetric, absolute instability remains unstable for the entire range of external pressures investigated. These results are consistent with the experimental observations that compliant tubes collapse non-axisymmetrically under the influence of high external pressure but blow out symmetrically under sufficiently low external pressure.

In the range of wavenumbers where all three modes are unstable, the ratio between the high and low frequencies is conserved for all Reynolds numbers. However, this ratio changes slightly when the characteristic propagation speed of the viscoelastic medium does not match the characteristic flow speed, i.e. for very high or very low values of $\Gamma$. The frequency of the high frequency mode is less than three times that of the other two modes at high wavenumbers. However, at the most unstable wavenumbers, the frequency of mode *I* is three times that for modes *LD* and *LU*, in excellent agreement with experimental observations. Increasing the thickness of the elastic wall or its viscosity stabilizes the convective and absolute instability modes. Dissipation in the solid has the strongest effect on the high-frequency mode *I*, but the tube thickness has the weakest effect on that same mode.

While maintaining the constant-diameter-tube assumption, the present linear analysis should be extended to nonlinear one. Conditions under which the nonlinear dynamical system becomes chaotic will be of great practical interest. Finally, variable-diameter tubes are much more complex to analyze as compared to the present constant-diameter tubes, but such analysis will be a very worthwhile endeavor. Perhaps one can start with a steady basic flow in a convergent–divergent tube. Linear stability analysis of this basic flow can then be conducted to find the resulting instability modes and compare them to the present constant-diameter modes. The model complexity can be gradually increased to ultimately solve a realistic collapsible tube problem using only first principles.

## REFERENCES

Bertram, C.D., and Castles, R.J. (1999) "Flow limitation in uniform thick-walled collapsible tubes," *J. Fluids & Structures* **13**, pp. 399–418.

Bertram, C.D., and Godbole, S.A. (1995) "Area and pressure profiles for collapsible-tube oscillations of three types," *J. Fluids & Structures* **9**, pp. 257–277.

 Copyright © 2001 by ASME

Carpenter, P.W. (1998) "Current status of the use of wall compliance for laminar-flow control," *Exp. Thermal & Fluid Sci.* **16**, pp. 133–140.

Gad-el-Hak, M. (1986) "Boundary-layer interactions with compliant coating: An overview," *Appl. Mech. Rev.* **39**, pp. 511–524.

Hamadiche, M. (1998) "Instabilité causée par l'interaction fluide/structure,'" in *34$^{eme}$ Colloque d'Airodynamique Appliqué de la A.A.A.F.*, 23–25 Mars, ESM2, Marseille, France.

Hamadiche, M., and Gad-el-Hak, M. (2001a) "Temporal stability of flow through viscoelastic tubes," *J. Fluids & Structures*, to appear.

Hamadiche, M., and Gad-el-Hak, M. (2001b) "Spatio–temporal stability of flow through collapsible, viscoelastic tubes," *J. Fluids & Structures*, to appear.

Heil, M. (1997) "Stokes flow in collapsible tubes: computation and experiment," *J. Fluid Mech.* **353**, pp. 285–312.

Huerre, P., and Monkewitz, P.A. (1990) "Local and global instabilities in spatially developing flows," *Annu. Rev. Fluid Mech.* **22**, pp. 473–537.

Kounanis, K., and Mathioulakis, D.S. (1999) "Experimental flow study within a self oscillating collapsible tube," *J. Fluids & Structures* **13**, pp. 61–73.

Kupfer, K., Bers, A., and Ram, A.K. (1987) "The cusp map in the complex-frequency plane for absolute instabilities," *Phys. Fluids* **30**, pp. 3075–3082.

Landahl, M.T. (1962) "On the stability of a laminar incompressible boundary layer over a flexible surface," *J. Fluid Mech.* **13**, pp. 609–632.

Luo, X.Y., and Pedley, T.J. (2000) "Multiple solutions and flow limitation in collapsible channel flows," *J. Fluid Mech.* **420**, pp. 301–324.

Scott, M.R., and Watts, H.A. (1977) "Computational solution of linear two-point boundary value problems via orthonormalization," *SIAM J. Numerical Analysis* **14**, pp. 40–70.

Shapiro, A.H. (1977) "Steady flow in collapsible tubes," *J. Biomech. Engng.* **99**, pp. 126–147.

Yeo, K.S., Khoo, B.C., and Zhao, H.Z. (1999) "The convective and absolute instability of fluid flow over viscoelastic compliant layers," *J. Sound & Vibration* **223**, pp. 379–398.


Copyright © 2001 by ASME